Title

Change in Cone Structure Over 24 Months in USH2A-Related Retinal Degeneration

Authors

Duncan, Jacque L
Liang, Wendi
Maguire, Maureen G
et al.

Publication Date

2023-08-01

DOI

10.1016/j.ajo.2023.03.006

Peer reviewed

HHS Public Access

Author manuscript

Am J Ophthalmol. Author manuscript; available in PMC 2024 August 01.

Published in final edited form as:

Am J Ophthalmol. 2023 August ; 252: 77–93. doi:10.1016/j.ajo.2023.03.006.

Change in Cone Structure Over 24 Months in *USH2A*-Related Retinal Degeneration

JACQUE L. DUNCAN,
WENDI LIANG,
MAUREEN G. MAGUIRE,
TRAVIS C. PORCO,
JESSICA WONG,
ISABELLE AUDO,
JENNA A. CAVA,
KATE GRIEVE,
ANGELOS KALITZEOS,
JOSEPH KREIS,
MICHEL MICHAELIDES,
NATHANIEL NORBERG,
MICHEL PAQUES,
JOSEPH CARROLL

University of California, San Francisco, CA, USA; Jaeb Center for Health Research, Tampa, FL, USA; *Quinze Vingts* National Ophthalmology Hospital, Paris, France; Medical College of Wisconsin, Milwaukee, WI, USA; Moorfields Eye Hospital, London, UK

FOUNDATION FIGHTING BLINDNESS CONSORTIUM INVESTIGATOR GROUP

Abstract

PURPOSE: To describe cone structure changes using adaptive optics scanning laser ophthalmoscopy (AOSLO) in the Rate of Progression of *USH2A*-related Retinal Degeneration (RUSH2A) study.

DESIGN: Multicenter, longitudinal natural history study.

Inquiries to Jacque L. Duncan, Wayne and Gladys Valley Center for Vision, 490 Illinois St, #53A, University of California, San Francisco, San Francisco, CA 94158, USA; jacque.duncan@ucsf.edu.

Author contributions: J.L.D., J.C., T.C.P., and M.M. designed and conducted the study. J.L.D., J.C., T.C.P., M.M., J.K., J.W., J.C., A.K., K.G., N.N., M.P., I.A., M.M., and A.A. collected, managed, analyzed, and interpreted the data. J.L.D., J.C., A.A., T.C.P., M.M., J.K., J.W., J.C., A.K., K.G., N.N., M.P., I.A., M.M., and A.A. and prepared, reviewed, or approved the manuscript. All authors attest that they meet the current ICMJE criteria for authorship.

Financial Disclosures: Jacque L. Duncan has been a consultant for AGTC Therapeutics, Biogen, California Institute for Regenerative Medicine, Conesight, DTx Therapeutics, Foundation Fighting Blindness, Editas Medicine, Gyroscope, Helio, Nacuity, ProQR Therapeutics, PYC Therapeutics, SparingVision, Spark Therapeutics, and Vedere Bio.

Conflicts of Interest: All authors have completed and submitted the ICMJE form for disclosure of potential conflicts of interest.

Supplemental Material available at AJO.com.

METHODS: AOSLO images were acquired at 4 centers, twice at baseline and annually for 24 months in this natural history study. For each eye, at least 10 regions of interest (ROIs) with ≥50 contiguous cones were analyzed by masked, independent graders. Cone spacing Z-scores, standard deviations from the normal mean at the measured location, were compared between graders and tests at baseline. The association of cone spacing with clinical characteristics was assessed using linear mixed effects regression models weighted by image quality score. Annual rates of change were calculated based on differences between visits.

RESULTS: Fourteen eyes of 14 participants were imaged, with 192 ROIs selected at baseline. There was variability among graders, which was greater in images with lower image quality score ($P < .001$). Cone spacing was significantly correlated with eccentricity, quality score, and disease duration ($P < .02$). On average, the cone spacing Z-score increased 0.14 annually (about 9%, $P < .001$). We observed no significant differences in rate of change between disease type (Usher syndrome or retinitis pigmentosa), imaging site, or grader.

CONCLUSIONS: Using current methods, the analysis of quantitative measures of cone structure showed some challenges, yet showed promise that AOSLO images can be used to characterize progressive change over 24 months. Additional multicenter studies using AOSLO are needed to advance cone mosaic metrics as sensitive outcome measures for clinical trials.

INHERITED RETINAL DEGENERATION (IRDs) ARE AMONG the most challenging diseases seen by ophthalmologists. They are genetically heterogeneous, associated with hundreds of variants in over 280 genes.[1] In addition, IRDs are clinically heterogeneous wherein changes in the same gene can produce a wide range of retinal and systemic phenotypes, even in individuals with the same pathogenic variants.[2-6] To date, only gene augmentation involving a single genetic defect for early onset retinal degeneration associated with variants in *RPE65* has received regulatory approval as gene therapy.[7,8]

Following the success of developing an approved treatment for *RPE65*-related retinal degeneration, ≥30 clinical trials of gene augmentation are underway for a number of IRDs (www.clinicaltrials.gov). However, several clinical trials that showed promise in phase 2 studies paused enrollment after they failed to meet prespecified primary outcome measures of safety and efficacy, including gene augmentation with timrepigene emparvovec for choroideremia (NCT03496012), cotoretigene toliparvovec for *RPGR*-related X-linked retinitis pigmentosa (NCT03116113), and antisense oligonucleotide therapy with sepofarsen for c.2991+1655A>G, p.Cys998X *CEP290*-related LCA10 (NCT03913143). These challenges have stimulated interest in leveraging natural history studies to identify patients who retain structure and/or function and may be most likely to benefit from treatment, and to guide selection of outcome measures that are most likely to demonstrate safety and efficacy during clinical trials lasting ≥24 months.

The development of therapies for patients with other IRDs has been challenging because these diseases progress slowly, and standard outcome measures of safety and efficacy are insensitive indicators of disease progression for patients with IRDs.[9-11] The slow rate of progression over decades in patients with IRDs is hard to measure quantitatively during the timeframe of a typical clinical trial lasting 1-3 years.[12-14] Measures of photoreceptor function are variable and affected by features seen in patients with retinal degenerations that

are not directly related to photoreceptor survival, including cystoid macular edema, cataract, epiretinal membrane, refractive error, fixation instability, and even patient attention. In primary rod degenerations such as retinitis pigmentosa (RP) and Usher syndrome, standard measures of visual function such as visual acuity are preserved until late in the disease process, and although static and kinetic perimetry thresholds change earlier, these responses can be variable.[12-16] More sensitive measures such as fundus-guided microperimetry may be complicated by unsteady fixation or inability to perform the test reliably.[17] Dark adaptation is required to measure the earliest changes in rod function with full-field stimulus threshold testing[18] and dark-adapted perimetry.[19] Clinically relevant measures of visual function such as mobility testing are resource-intensive, requiring space and several hours to conduct,[20] and most patient-reported outcome questionnaires have not been validated for specific retinal degenerations.[21,22] Objective measures of photoreceptor function such as full-field and multifocal electroretinography may require contact with the cornea, demonstrate quantifiable change only when large amounts of photoreceptors have been lost, and are influenced by dilation, fixation, and blink artifact.[16,23] For all these reasons, objective, quantifiable measures of IRD severity and progression are urgently needed to facilitate clinical trials of new therapies for these conditions.

Although high magnification can improve image resolution, most standard clinical images of retinal structure such as optical coherence tomography (OCT) lack sufficient lateral resolution to distinguish rod from cone photoreceptors.[24,25] Adaptive optics (AO) is a strategy to improve retinal image resolution by compensating for wavefront aberrations.[16,23,26,27] Commercially available flood-illuminated systems incorporate AO correction into a fundus camera, but have limited resolution within 2 degrees of the foveal center.[28,29] AO correction of scanning laser ophthalmoscope (AOSLO) images with confocal and split modalities permits visualization of individual photoreceptors in the macula and disambiguation of cone from rod photoreceptors,[16,30] including in *USH2A*-related retinal degeneration.[31] Several measures of AOSLO cone images have been reported at regions of interest (ROIs) where unambiguous cones are identified, including cone spacing or average nearest neighbor distance.[32] The distance between cones can indicate cone loss with retinal degeneration; cone spacing is a robust and conservative measure that may be insensitive to detecting small changes over time. However, where image quality is imperfect, it is less variable than cone density, which requires unambiguous identification of every cone in the mosaic.[32] Cone spacing varies predictably with distance from the fovea,[33,34] with lowest cone spacing (greatest cone density) at the fovea, increasing exponentially within 5 degrees of the foveal center; cone densities are greater along the horizontal compared with the vertical meridian.[35] Measures of cone structure integrity include cone spacing Z-scores (number of standard deviations from the normal mean at the measured location), cone packing regularity, and number of ROIs separated at regular intervals where cones can be unambiguously identified.[32,36] AOSLO images have been used to monitor changes in average cone spacing longitudinally over 2-3 years in small numbers of patients with rod-cone degenerations,[36,37] and can reveal changes that are not detectable using OCT or other imaging modalities.[38-40] However, to date AOSLO has not been used to measure photoreceptor degeneration in multicenter, longitudinal natural history or clinical treatment trials of IRD patients.

Variants in *USH2A* are the most common genetic cause of Usher syndrome type 2 (USH2) and nonsyndromic autosomal recessive RP (ARRP).[41] *USH2A* exceeds the carrying capacity of adeno-associated viral vectors, spanning 800 kb,[42] but clinical trials are planned or underway to develop antisense oligonucleotide (NCT05158296) and other gene editing or augmentation treatments for this common cause of rod-cone degeneration. The Rate of Progression of *USH2A*-Related Retinal Degeneration (RUSH2A; NCT03146078) study is a multicenter, international, longitudinal natural history study[15] designed to identify and validate outcome measures of disease progression in patients with *USH2A*-related retinal degeneration. The RUSH2A study is collecting clinical data at 16 sites in 4 countries on the rate of photoreceptor degeneration in patients with 2 pathogenic or likely pathogenic variants in *USH2A*.[2] However, the standard clinical tests included in the protocol do not have the resolution necessary to study cone photoreceptor structure on a cellular level. No published studies to date have characterized the longitudinal change in cone structure over time in eyes with *USH2A*-related retinal degeneration[31] or correlated that information with standard clinical measures of retinal structure or function. The present study used AOSLO imaging to test the hypothesis that cone topography (ie, cone spacing and density) will show significant change from baseline to 2 years in patients with *USH2A*-related retinal degeneration. In the RUSH2A study, patients with USH2 showed more severe disease progression compared with nonsyndromic ARRP[15,18] at baseline, adjusting for age at enrollment and duration of disease; truncating alleles in *USH2A* were more likely associated with hearing loss in USH2, while a group of missense alleles were associated with milder vision loss in ARRP.[2] The present study will test the hypothesis that measures of cone spacing and density will show differences in rates of change over 2 years between patients with USH2 and ARRP caused by variants in *USH2A*.

METHODS

SUBJECTS:

Candidates for the present longitudinal, observational AOSLO study were a subset of participants enrolled in the RUSH2A study (NCT03146078) at 16 clinical sites in Europe and North America. Only participants enrolled at the 4 sites with AOSLO systems were eligible for the current study. The ethics boards at each site approved the AOSLO and RUSH2A study protocols, and the study adhered to the tenets of the Declaration of Helsinki. The overall RUSH2A study design and inclusion and exclusion criteria were reported previously.[15] Briefly, all participants had rod-cone degeneration with biallelic disease-causing variants in *USH2A*. Candidates for the current study were recruited from the participants in cohort 1 of the RUSH2A study, with best-corrected visual acuity (BCVA) of ≥54 letters using the Early Treatment of Diabetic Retinopathy Study protocol,[43,44] ≥10 degree diameter kinetic visual field to the III4e isopter (Octopus 900 Pro, Haag Streit), and stable fixation in the eye with better visual acuity, which was chosen as the study eye for longitudinal follow up annually over 4 years.[15] Disease duration was based on age of onset of visual symptoms reported by participants.

AOSLO ELIGIBILITY CRITERIA:

Clinical staff at study sites with AOSLO capability (Medical College of Wisconsin, University of California San Francisco, Moorfields Eye Hospital, and the Quinze Vingts National Ophthalmology Hospital) reviewed the RUSH2A AOSLO manual of procedures for obtaining AOSLO montages and AOSLO imaging and were certified by the RUSH2A Coordinating Center. Participants in the RUSH2A study without corneal or lens opacity, nystagmus, unsteady fixation, or dry eye in the study eye[15] were invited to provide written informed consent for the RUSH2A AOSLO ancillary study.

AOSLO IMAGE ACQUISITION AND ROI SELECTION:

Initial baseline AOSLO images were acquired twice within 60 days of the RUSH2A 12-month study visit. Each AOSLO montage spanned a region that was at least 5 × 5 degrees, centered on the fovea, and extended superiorly and inferotemporally along the regions imaged with horizontal and vertical OCT B-scans until a large vessel was imaged, to facilitate alignment with infrared fundus images acquired simultaneously with OCT and microperimetry, and color fundus photographs (Figure 1, A). Confocal and split detector AOSLO images were acquired simultaneously at each location with pixel sampling density no less than 400 pixels/degree. Montages were assembled using shared custom software,[45] superimposed on color fundus photos and aligned with horizontal and vertical OCT B-scans through the fovea (Adobe Illustrator, Adobe, San Jose, California, USA) (Figure 1), and submitted to a server that was General Data Protection Regulation– and Health Insurance Portability and Accountability Act–compliant for review by the AOSLO coprincipal investigator (J.C.) who was masked to clinical information about the participants. Participants were required to have ≥10 ROIs separated by roughly 1-degree intervals across the montage, each containing contiguous patches of ≥50 unambiguous cones arranged in mosaics on both baseline visits to be included in the AOSLO RUSH2A study. Ten ROIs were required at baseline with the goal of retaining measurable cones at >5 of the original ROIs after 36 months. AOSLO imaging was repeated once annually within 60 days of the RUSH2A 24- and 36-month visits to provide AOSLO follow-up at 12 and 24 months. Baseline ROIs were at locations where the ellipsoid zone band was visible on OCT B-scans, avoiding regions with cystoid spaces or inner retinal opacification that could obscure visualization of cones, within 10 degrees of the foveal center. ROI size ranged from 0.35 × 0.35 degrees to 0.5 × 0.5 degrees, increasing with eccentricity to include 50 unambiguous cones in the mosaic; the maximum number of ROIs that included 50 unambiguous cones per eye were included. For each participant, ROIs were selected from their follow-up AOSLO montages at the same retinal locations as were used at baseline (using the ROI pattern exported from Mosaic Analytics depicted in Figure 1).

ASSESSING CONE STRUCTURE:

At least 2 trained and masked independent graders identified cone locations at the ROIs using custom software (Mosaic Analytics, Translational Imaging Innovations, Inc., Hickory, North Carolina, USA) to calculate cone spacing (average nearest neighbor distance in microns) based on the density recovery profile method,[46] and cone density, or total number of cones with bound Voronoi domains divided by the sum of the Voronoi domain area in

mm^2, which was measured at ROIs where every cone in the mosaic was unambiguously identified. Raw coordinates were in pixel space. Conversions to microns or arcminutes were based on the calibrated scale of the AOSLO system used to acquire the image in pixels/degree and the assumption of 291 μm/degree for a 24-mm eye, scaled by each subject's axial length. Each grader provided an image quality score ranging from 0-5, representing ungradable (0) to high confidence (5) in cone identification, that represented the confidence the grader had in marking the cone locations. Any ROI where the cone spacing measures from either grader had a confidence level of 0 was flagged for adjudication. If the independent adjudicator (J.L.D.) agreed that the image was ungradable (containing <50 unambiguous cones), the data for that grader were not used for that ROI. If the adjudicator disagreed with the level of 0, the adjudicator completed the grading according to the same procedures for graders to determine cone metrics as described above, and the adjudicator's assessment super-seded the original grading for the specific ROI. Images from all visits were measured in random order to minimize the impact of learning effects. Retinal vascular landmarks were used to align montages with baseline images so the ROIs identified at baseline could be identified and cones counted at each follow-up image. Graders were allowed to adjust the contrast of the image to improve cone visualization.

STATISTICAL ANALYSIS:

To account for the relationship between cone spacing and eccentricity (distance from the foveal center),[33] cone spacing measures were converted to Z-scores, or standard deviations from the mean cone spacing measured at that same location in 40 normal eyes, ranging in age from 18-82 years (mean 33.6 years; standard deviation [SD] 13.7 years). Data of 28 eyes was taken from Wang et. al., for higher resolution images of foveal cones.[55] Z-scores were calculated from curves fit to the normal cone spacing data at each eccentricity from the foveal center.

To calculate approximate Z-scores from cone spacing measurements, we modeled the mean spacing μ as a function of location using a model. For horizontal and vertical directions i = 1,2, we calculated μ_i according to the double exponential $\mu_i = b_i e^{-c_i \gamma_i} + f_i e^{-g_i \gamma_i}$ where γ_i is the horizontal or vertical coordinate of the ROI. We then assumed an elliptical dependence to calculate $\mu = \frac{\mu_1 \mu_2}{\sqrt{(\mu_1 \cos\theta)^2 + (\mu_2 \sin\theta)^2}}$ (where θ is the angle between the positive x-axis and the ray subtended between the foveal center and the ROI). In addition, we modeled the standard deviation about this non-linear regression line according to $\sigma = e^{a_1 + a_2 \mu}$. In practice, we assumed $g_1 = g_2$, giving a total of 9 parameters to fit. We used the Nelder-Mead downhill simplex algorithm[47] for fitting, choosing 12 different randomly chosen initial values. For our data, we found evidence that $a_2 \neq 0$, implying a standard deviation that varies with the mean value μ. As a sensitivity analysis, however, we calculated alternative Z-scores under the assumption that $a_2 = 0$ as well (thus assuming a constant conditional standard deviation at each location, results not shown).

The distribution of AOSLO cone spacing (arcminutes and Z-scores) and cone density measures at each visit was summarized using means, SDs, medians, interquartile ranges (IQRs), and ranges. Linear mixed effects regression models with weighting based on image

quality score were used to estimate the annual rates of change and evaluate the association between baseline participant characteristics with cone spacing Z-score at each ROI. Weights based on image quality score were calculated using the reciprocal of the root mean square between graders. We accounted for the similarity of ROIs within each eye using a random effect, and we included an additional crossed random effect for each ROI to account for the longitudinal follow-up in each ROI, clustering effect by individual, multiple ROIs. The grader was adjusted for in all the analysis models as a fixed variable. Mixed effects models were fit using maximum likelihood estimation (using the lme4 package in R); statistical assessment of regression coefficients was conducted using the Wald test.[48] Time in years was calculated as the number of days from the baseline AOSLO (RUSH2A 12-month) visit divided by 365.25 for the longitudinal analysis. The methods of Bland and Altman for assessing agreement between measurements were used to assess variability of baseline repeated test measures and intergrader agreement.[49] Intergrader disagreement was also evaluated using a mixed effects model with grader as a predictor of the Z-score.

Associations between cone spacing Z-score and other clinical measures of disease severity (BCVA measured as letters read using a standardized eye chart and protocol),[43,44] dark-adapted full-field stimulus threshold to blue, red, and white stimuli (Espion e3, Diagnosys LLC, Lowell, Massachusetts, USA) measured as described previously,[18] and fundus-guided mesopic microperimetry, tested using a Macular integrity Assessment (MAIA-2) system (Center-Vue, Padova, Italy; microperimetry mean sensitivity was averaged over responses from a circular grid of 89 points centered on the fovea and extending to the temporal arcades, as described previously). Ellipsoid zone (EZ) area was measured at baseline from 121 spectral-domain OCT B-scans within a 30- by 25-degree retinal area centered on the fovea with automatic real-time tracking of 9 (Spectralis HRA+OCT, Heidelberg Engineering GmbH, Heidelberg, Germany), as follows. The Duke Optical Coherence Tomography Retinal Analysis Program was used to manually annotate A-scans with intact EZ on each B-scan from OCT macular volumes, and to calculate the intact EZ area. Readers first annotated the foveal B-scan, where the intact EZ is easier to identify, then annotated the neighboring B-scans. In borderline cases in which the presence or absence of the EZ was not clear, the reader assumed EZ continuity from the fovea. A second senior reader reviewed all B-scan gradings of the first reader and corrected the gradings when needed. To correlate with other clinical measures, cone spacing Z-scores were averaged among all ROIs within each study eye. Correlation between average cone spacing Z-scores and the clinical measures from baseline to 2 years was assessed with Spearman correlation coefficients. Bonferroni-Holm adjustment was used for the Spearman coefficients.[50] All analyses were conducted using R (version 3.5.1) and SAS software (version 9.4, SAS Institute, Cary, North Carolina, USA). All reported *P* values and 95% confidence intervals (CIs) were 2-sided.

Using Z-score as an outcome, we assessed several predictors. At the patient level, we included project site, sex, and disease duration other redictors were grader, test number, eccentricity, the number of ROIs at each visit, and quality score. Random effects were included for each ROI and patient, as described above. Duration of disease was computed based on age of onset and date of enrollment. No adjustments for multiplicity were made.

RESULTS

STUDY POPULATION:

From the 105 participants enrolled in the RUSH2A primary cohort, 34 were enrolled at sites with AOSLO systems and 32 of 34 consented to AOSLO imaging (Figure 2). Eight consenting participants did not have 2 baseline AOSLO images obtained, due to cataract (n = 2), corneal opacity or lack of optical clarity (n = 1), fatigue with refusal to undergo second AOSLO baseline imaging session (n = 3), being <18 years of age at the time of AOSLO imaging (n = 1), or AOSLO system malfunction (n = 1). Among the 24 participants that completed initial AOSLO testing, 10 were discontinued due to not meeting the study inclusion criteria (≥10 ROIs each with ≥50 cones and separated by approximately 1-degree intervals in the central retina) upon review by an independent, experienced AOSLO expert (J.C.). Fourteen participants completed both baseline visits, 12 completed the 1-year visit, and 14 completed the 2-year visit. Two participants missed the 12-month (RUSH2A 24-month visit) visit, 1 due to equipment malfunction, the other during 2020 when nonessential clinical research visits were prohibited during the COVID-19 pandemic.

Three graders measured cone spacing from all baseline visits. Because 1 grader relocated and was no longer available to grade the remaining images, all cone spacing measures from the 24-month visits were measured by the remaining 2 graders. A total of 30 ROIs from 4 participants were judged to be ungradable with image quality score = 0; all 30 were reviewed, confirmed to be ungradable by the adjudicator, and were not included in the analysis.

Clinical characterization of participants is shown in Table 1. Among the 14 participants, the clinical diagnosis was USH2 for 6 (43%) participants and ARRP for 8 (57%) participants. The mean age was 38 years (range 19-59 years), 11 (79%) were white, and 10 (71%) were male. The age of onset of disease reported by the participant was younger in the USH2 group than in the ARRP group (median 14 vs 39 years). The USH2 participants had relatively longer duration of disease than ARRP participants (median 14 vs 6 years). One grader measured cone spacing from all baseline visits, all 12-month visits, and 53% of the 24-month visits before leaving the project. Since the dataset from this grader was only complete at baseline, the only values that were used for this grader were from baseline in the analysis of intervisit variability at baseline (grader 2, Table 2).

INTERTEST COMPARISONS:

Bland-Altman plots (Figure 3) showed no significant difference in mean cone spacing (microns) between test 1 and test 2 at baseline (95% limits of agreement included 0). The average Z-score for test 1 and test 2 equaled 1.37 and 1.36, respectively (SDs 2.48 and 2.61, $P = .93$). Image quality scores at the second baseline visit (mean [SD], 2.58 [1.03]) were significantly lower than the first baseline visit (mean [SD], 2.67 [1.00], $P = .007$).

INTERGRADER COMPARISONS:

At baseline, grader 2 generated consistently lower scores than graders 1 and 3 (Table 2 Supplemental Figure 1, $P < .001$). Intergrader variation as measured by Z-score difference

was greater at ROIs with image quality scores of 1 and 2 vs high-quality images with scores from 3-5 (median 1.50 vs 1.18 vs 0.69, respectively; $P < .001$). At all visits, the mean difference between grader 1 and 3 centered around 0 and showed high concordance (Supplemental Figure 2).

CONE SPACING (Z-SCORE):

The cone density and cone spacing values from, baseline to 24 months are summarized in Table 3. Cone spacing had a significant negative correlation with cone density (−0.74 [95% CI −0.76 to −0.71]). The mean (SD) Z-score for cone spacing increased from 1.57 (2.61) to 1.80 (2.78) from baseline to 24 months. Cone spacing (not converted to Z-score) did not change over time (mean 1.38, 1.39, and 1.37, respectively). Greater average cone spacing (not converted to Z-score) was associated with greater eccentricity ($P < .001$, Figure 4). At baseline, cone spacing Z-scores were greater in patients with USH2 (mean [SD], 2.14 [3.05]) than ARRP (mean [SD], 1.20 [2.19]), but the difference was not statistically significant (Table 3). Participants with fewer regions that had gradable cones had significantly lower quality scores than those with more regions at baseline (Table 4). Cone spacing Z-score decreased significantly with eccentricity and image quality score but increased with disease duration (Table 5). In the weighted model, no significant difference was observed in baseline cone spacing Z-score based on clinical diagnosis, gender, test number, number of ROIs, or imaging site.

Although participants with <10 ROIs at baseline were not eligible to participate, the number of ROIs in each subject ranged from 10 to >15 at baseline and declined at 12- and 24-month visits; by 24 months of follow-up, 4 of 14 (31%) montages had <10 ROIs remaining (Table 4). Although 6 of 14 (46%) montages imaged at 24 months had all the ROIs that were present at baseline, 4 of 14 (31%) had lost between 4-7 of the original ROIs by the 24-month visit (Table 4). The average image quality score was lower in montages with 10 ROIs than montages with >20 ROIs at baseline (Table 4). The mean number of ROIs decreased from 13.7 to 11.6 from baseline to the 24-month visit ($P = .01$), and the mean quality score decreased from 2.48 to 2.15 from baseline to 24 months ($P = .01$). However, there was no correlation between decrease in quality score overtime with baseline number of ROIs ($P = .09$).

Cone spacing Z-score increased during longitudinal follow-up (Table 3 and Figures 5 and 6). The estimated average annual change in cone spacing Z-score, weighted by quality score and disease duration, increased by 0.14 (95% CI 0.07-0.21, $P < .001$) (Table 6). A significant association was found between the number of ROIs and Z-score over time: patients with fewer ROIs had greater annual increase in Z-score (Table 6). Examples of change at ROIs which showed an increase in cone spacing (Figure 7, A), no change in cone spacing (Figure 7, B) and a decrease in cone spacing (Figure 7, C) are shown in Figure 7.

Mean cone spacing Z-score in each montage was not significantly correlated with BCVA, full-field stimulus threshold, microperimetry mean sensitivity, or OCT EZ area, at baseline and across all time points, adjusted for multiple comparisons (Table 7).

Results were not substantially changed using an alternative Z-score based on the model with constant standard deviation, described in the Methods section.

DISCUSSION

In the present study, we observed a significant increase in cone spacing Z-score over 24 months (+0.14 [95% CI, 0.07 to 0.21], $P < 0.001$) and observed a significant reduction of gradable ROIs with remaining cones (−0.18 ROIs/year [95% CI, −0.23 to −0.12], $P < 0.001$). The change of +0.14 in Z-score is small in magnitude but statistically significant over 24 months. Although structural measures such as EZ width have shown significant change in patients with X-linked RP, because the repeat variability of ellipsoid zone width was lower than the annual rate of change,[51] most studies have not demonstrated a significant change in functional measures of disease progression such as kinetic or static perimetry or microperimetry over 24 months. We did not find a significant difference between USH2 and ARRP participants at baseline, or in the rate of change, perhaps because the sample size was small, resulting in low power to detect differences in rates of change between the 2 groups over 24 months.

The present study is the first to investigate AOSLO cone spacing measures as an outcome measure of disease progression in a multicenter natural history study of *USH2A*-related IRD. Despite challenges associated with image acquisition at different sites using different AOSLO systems, we observed no significant difference between the cone spacing in images acquired at different locations (Table 4). To investigate intervisit variability, we obtained AOSLO images at 2 sessions separated by ≤60 days at baseline. Image quality scores at the second baseline visit (mean [SD], 2.58 [1.03]) were significantly lower than the first baseline visit (mean [SD], 2.67 [1.00], $P = .007$). The requirement to obtain 2 baseline images was intended to increase the likelihood that selected ROIs would be of sufficient image quality to remain useful at follow-up visits. However, our results suggest that there is no added benefit to collecting a second AOSLO image at baseline. The requirement for 2 montages with ≥10 gradable ROIs at baseline resulted in exclusion of 10 of 24 screened subjects and required, in some cases, an extra day of testing. The inclusion requirement that each eligible montage at baseline had ≥10 gradable ROIs was intended to increase the likelihood that ≥5 gradable ROIs would remain at 36 months after baseline AOSLO imaging. Screen failures with <10 ROIs during both baseline imaging sessions resulted from media opacity, unsteady fixation, tear film abnormalities, patient fatigue or refusal to return for a second imaging session, cystoid macular edema, and high refractive error, all of which may be associated with more severe photoreceptor degeneration. Figure 7, C shows examples in which the cone spacing decreased at 24 months compared with baseline, likely because the image quality improved at the later visit. The requirement of 2 baseline imaging sessions with 10 gradable ROIs at baseline likely biased the results presented to include patients with earlier stages of degeneration and better cone structure at the beginning of the study. Future studies should not require >1 baseline image, as additional imaging sessions yielded lower image-quality scores, may increase fatigue, and could compromise test performance of other studies. In this small study, we weighted cone spacing values by image quality score to give less value to images where graders had lower confidence in their cone identifications. This permitted inclusion of as much data as possible.

Cone spacing in the current study was measured by trained, independent graders who were masked to clinical diagnosis and measures of disease severity. We observed significant differences between graders, which has also been reported in quantitative studies of AOSLO in patients with achromatopsia.[52] For this reason, our analysis of longitudinal change in cone spacing at each ROI was clustered by grader to compensate for bias between graders. Variation between graders was greatest for ROIs with lower image quality scores where graders had lower confidence in their cone identifications. We plan to analyze internal consistency within each grader at the end of the RUSH2A study by requiring each grader to regrade 10% of all ROIs in random order.

In eyes with retinal degeneration, the expectation is that cones may be lost due to disease progression over the course of a longitudinal study. We did not attempt to identify and track individual cones over time for this reason. Small misalignments of the ROIs between timepoints could contribute to errors in estimating the amount of change at a specific cone mosaic locus. ROI alignment issues may be avoided by moving away from ROI-based analyses and using more continuous measures across a mosaic, though additional computational tools would be needed to help make that a reality.

Larger cone spacing was associated with greater eccentricity, which is consistent with histologic studies.[33] In the present study, eccentricity was significantly associated with Z-score, but the most abnormal cone spacing was observed closest to the fovea rather than at the greatest eccentricities imaged. The Z-score measure depends on cone spacing in arcminutes at the ROI, and the mean cone spacing in arcminutes from normal subjects imaged at the same distance from the fovea. The size, accuracy, and comparability of the reference data is as important as the fidelity of the measure from the ROI being assessed in deriving the Z-score for each ROI. Greater Z-scores near the fovea in participants with *USH2A*-related retinal degeneration observed in the current study may reflect more severe cone loss near the fovea or may result from a small range of cone spacing values observed in normal participants within 0.5 degrees of the foveal center. This possibility led us to investigate 2 different methods to estimate Z-scores, one which incorporated the variance in normal data at each location studied, and an alternate method in which the variation was fixed at all locations; we observed the same result using both approaches with greater evidence of cone loss near the fovea and better cone preservation farther from the fovea. The observed result may reflect preservation of ROIs at greater eccentricities in participants who had earlier disease (with lower Z-scores), while patients with more advanced disease retained ROIs only near the foveal center. To test this hypothesis, we compared the number of ROIs at baseline with the change in Z-score over time and found no significant correlation (Table 4), however. Alternatively, the larger differences in Z-score close to the fovea may reflect slight inaccuracies in precise alignment of the montages from each time point. Small misalignments in ROIs between timepoints would result in a greater “change” in density near the fovea due to the high density of foveal cones and rapid decline in cone density with eccentricity. The “anchor” against which ROI location was derived may need to be re-evaluated in future trials and efforts to align the montages should be explored.[53,54]

Lastly, some ROIs that were included based on both baseline montages were not seen at subsequent visits. There are several reasons that ROIs may be lost during follow-

up, including loss of cone structure as a consequence of disease progression; reduced image quality at follow-up visits due to cataract, tear film abnormality, posterior capsular opacification, or cystoid macular edema; and failure to capture images of sufficient quality to count cones at every ROI on subsequent visits. Future studies using AOSLO should train AOSLO imaging personnel to review ROIs selected in baseline montages during image acquisition to ensure that retinal landmarks surrounding each ROI are imaged, and work to acquire the highest possible quality images at each subsequent visit.

A limitation of using AOSLO images to monitor disease progression is common to all outcome measures in that they can only be measured where visible structure remains. Therefore, AOSLO measures the best-preserved cones and is a conservative measure of disease progression, because cones that have degenerated are not visible, and cones undergoing degeneration may yield images that are ambiguous. In the present study, cone spacing increased, ROIs were lost, and image quality score decreased over 24 months. Since more advanced disease likely causes greater disruption of the cone mosaic with reduced confidence of cone markings, this may limit the utility of AOSLO images as a marker of disease progression in clinical trials of treatments for patients with more advanced disease, where other clinical measures such as perimetry or visual acuity could show change. However, multiple recent clinical trials of potential treatments for patients with IRD have been halted for failing to demonstrate significant decreases in the rate of disease progression based on standard clinical measures (NCT03496012, NCT03116113, and NCT03913143). Perhaps these recent failures occurred because the main outcome measures of the studies were not sufficiently sensitive to detect changes in the rate of progression in patients with earlier stages of disease during the 24-month trial duration. The current study demonstrated small, but statistically significant changes in cone spacing and in the number of remaining regions with measurable cones over 24 months.

This study demonstrated additional limitations in the use of AOSLO to measure progression in a clinical population. Ten of 24 screened patients did not have the required number of ROIs on both baseline imaging sessions, there was significant intergrader variability, and image quality score was worse in eyes with more severe disease progression. To use AOSLO measures of cone spacing in future clinical trials, it will be necessary to mitigate these factors in the following ways: (1) certifying >2 graders at the start of the study and analyzing data from all visits in random order contemporaneously at study completion with the same group of trained graders; (2) only using 1 baseline image; (3) ensuring that all ROIs imaged at baseline are captured at subsequent visits using retinal vascular landmarks to guide image acquisition; and (4) more precise ROI/montage alignment over time points. However, despite these limitations, the current study represents the first longitudinal, multicenter study using AOSLO images to monitor disease progression in patients with *USH2A*-related retinal degeneration. Over 24 months, cone spacing increased, indicating fewer cones remained compared with baseline at the measurable ROIs, and the number of ROIs with gradable cones decreased over 24 months. This finding suggests that cone spacing Z-score may be a sensitive measure of disease progression. The current results suggest AOSLO cone measures can detect, and may demonstrate, disease progression over 24 months, so may play an important role in phase 3 trials of that duration investigating safety and efficacy of novel compounds.

Supplementary Material

Refer to Web version on PubMed Central for supplementary material.

Funding/Support:

Funded by the Foundation Fighting Blindness, National Eye Institute grants U24 EY029891, R01EY023591, and P30 EY002162, Research to Prevent Blindness, Biogen/Nightstarx Therapeutics, Acucela, Allergan, and AGTC Therapeutics.

REFERENCES

1. Daiger SP. Summaries of genes and loci causing retinal diseases. Available at https://web.sph.uth.edu/RetNet/sum-dis.htm. Accessed December 22, 2022.
2. Hufnagel RB, Liang W, Duncan JL, et al. Tissue-specific genotype-phenotype correlations among USH2A-related disorders in the RUSH2A study. Hum Mum. 2022;43(5):613–624.
3. Rodríguez-Muñoz A, Aller E, Jaijo T, et al. Expanding the clinical and molecular heterogeneity of nonsyndromic inherited retinal dystrophies. J Mol Diagn. 2020;22(4):532–543. [PubMed: 32036094]
4. Zou X, Fu Q, Fang S, et al. Phenotypic variability of recessive *RDH12*-associated retinal dystrophy. Retina. 2019;39(10):2040–2052. [PubMed: 30134391]
5. Roshandel D, Thompson JA, Heath Jeffery RC, et al. Clinical evidence for the importance of the wild-type PRPF31 allele in the phenotypic expression of RP11. Genes (Basel). 2021;12(6):915. [PubMed: 34198599]
6. Pierrache LH, Hartel BP, van Wijk E, et al. Visual prognosis in USH2A-associated retinitis pigmentosa is worse for patients with Usher syndrome type IIa than for those with nonsyndromic retinitis pigmentosa. Ophthalmology. 2016;123(5):1151–1160. [PubMed: 26927203]
7. Daruich A, Boinet R, Falcou C, et al. Implementation of a new gene therapy in ophthalmology: regulatory and organizational issues [in French]. J Fr Ophtalmol. 2021;44(5):730–737. [PubMed: 33838946]
8. Collin RWJ, Garanto A. Preface of special issue "Molecular Therapies for Inherited Retinal Diseases. Genes (Basel). 2020;11(2):169. [PubMed: 32033431]
9. Ratnam K, Carroll J, Porco TC, Duncan JL, Roorda A. Relationship between foveal cone structure and clinical measures of visual function in patients with inherited retinal degenerations. Invest Ophthalmol Vis Sci. 2013;54(8):5836–5847. [PubMed: 23908179]
10. Foote KG, Loumou P, Griffin S, et al. Relationship between foveal cone structure and visual acuity measured with adaptive optics scanning laser ophthalmoscopy in retinal degeneration. Invest Ophthalmol Vis Sci. 2018;59(8):3385–3393. [PubMed: 30025078]
11. Bensinger E, Rinella N, Saud A, et al. Loss of foveal cone structure precedes loss of visual acuity in patients with rod-cone degeneration. Invest Ophthalmol Vis Sci. 2019;60(8):3187–3196. [PubMed: 31335944]
12. Fishman GA, Bozbeyoglu S, Massof RW, Kimberling W. Natural course of visual field loss in patients with type 2 Usher syndrome. Retina. 2007;27(5):601–608. [PubMed: 17558323]
13. Grover S, Fishman GA, Anderson RJ, Alexander KR, Derlacki DJ. Rate of visual field loss in retinitis pigmentosa. Ophthalmology. 1997;104(3):460–465. [PubMed: 9082273]
14. Iannaccone A, Kritchevsky SB, Ciccarelli ML, et al. Kinetics of visual field loss in Usher syndrome type II. Invest Ophthalmol Vis Sci. 2004;45(3):784–792. [PubMed: 14985291]
15. Duncan JL, Liang W, Maguire MG, et al. Baseline visual field findings in the RUSH2A study: associated factors and correlation with other measures of disease severity. Am J Ophthalmol. 2020;219:87–100. [PubMed: 32446738]
16. Duncan JL, Carroll J. Adaptive optics imaging of inherited retinal disease. Cold Spring Harb Perspect Med. 2022 a041285.

17. Lad EM, Duncan JL, Liang W, et al. Baseline microperimetry and OCT in the RUSH2A study: structure-function association and correlation with disease severity. Am J Ophthalmol. 2022;244:98–116. [PubMed: 36007554]
18. Birch DG, Cheng P, Duncan JL, et al. The RUSH2A study: best-corrected visual acuity, full-field electroretinography amplitudes, and full-field stimulus thresholds at baseline. Transl Vis Sci Technol. 2020;9(11):9.
19. Birch DG, Samarakoon L, Melia M, et al. The RUSH2A study: dark-adapted visual fields in patients with retinal degeneration associated with biallelic variants in the *USH2A* gene. Invest Ophthalmol Vis Sci. 2022;63(3):17.
20. Chung DC, McCague S, Yu ZF, et al. Novel mobility test to assess functional vision in patients with inherited retinal dystrophies. Clin Exp Ophthalmol. 2018;46(3):247–259. [PubMed: 28697537]
21. Durham T, Banhazi J, Patalano F, Jayasundera T. Beyond the NEI-VFQ: recent experience in the development and utilization of patient-reported outcomes for inherited retinal diseases. Cold Spring Harb Perspect Med. 2023;13(3) a041298. [PubMed: 36220332]
22. Lacy GD, Abalem MF, Andrews CA, et al. The Michigan Retinal Degeneration Questionnaire: a patient-reported outcome instrument for inherited retinal degenerations. Am J Ophthalmol. 2021;222:60–68. [PubMed: 32858027]
23. Wynne N, Carroll J, Duncan JL. Promises and pitfalls of evaluating photoreceptor-based retinal disease with adaptive optics scanning light ophthalmoscopy (AOSLO). Prog Retin Eye Res. 2021;83:100920. [PubMed: 33161127]
24. Wynne N, Heitkotter H, Woertz EN, Cooper RF, Carroll J. Comparison of cone mosaic metrics from images acquired with the SPECTRALIS high magnification module and adaptive optics scanning light ophthalmoscopy. Transl Vis Sci Technol. 2022;11(5):19.
25. Wade A, Fitzke F. A fast, robust pattern recognition asystem for low light level image registration and its application to retinal imaging. Opt Express. 1998;3(5):190–197. [PubMed: 19384360]
26. Roorda A, Williams DR. The arrangement of the three cone classes in the living human eye. Nature. 1999;397(6719):520–522. [PubMed: 10028967]
27. Roorda A, Duncan JL. Adaptive optics ophthalmoscopy. Annu Rev Vis Sci. 2015;1:19–50. [PubMed: 26973867]
28. Zaleska-Żmijewska A, Wawrzyniak ZM, Ulińska M, Szaflik J, Dąbrowska A, Szaflik JP. Human photoreceptor cone density measured with adaptive optics technology (rtxl device) in healthy eyes: standardization of measurements. Medicine (Baltimore). 2017;96(25):e7300. [PubMed: 28640147]
29. Feng S, Gale MJ, Fay JD, et al. Assessment of different sampling methods for measuring and representing macular cone density using flood-illuminated adaptive optics. Invest Ophthalmol Vis Sci. 2015;56(10):5751–5763. [PubMed: 26325414]
30. Scoles D, Sulai YN, Langlo CS, et al. In vivo imaging of human cone photoreceptor inner segments. Invest Ophthalmol Vis Sci. 2014;55(7):4244–4251. [PubMed: 24906859]
31. Gill JS, Theofylaktopoulos V, Mitsios A, et al. Investigating biomarkers for USH2A retinopathy using multimodal retinal imaging. Int J Mol Sci. 2022;23(8):4198. [PubMed: 35457016]
32. Cooper RF, Wilk MA, Tarima S, Carroll J. Evaluating descriptive metrics of the human cone mosaic. Invest Ophthalmol Vis Sci. 2016;57(7):2992–3001. [PubMed: 27273598]
33. Curcio CA, Sloan KR, Kalina RE, Hendrickson AE. Human photoreceptor topography. J Comp Neurol. 1990;292(4):497–523. [PubMed: 2324310]
34. Curcio CA, Sloan KR. Packing geometry of human cone photoreceptors: variation with eccentricity and evidence for local anisotropy. Vis Neurosci. 1992;9(2):169–180. [PubMed: 1504026]
35. Sawides L, de Castro A, Burns SA. The organization of the cone photoreceptor mosaic measured in the living human retina. Vision Res. 2017;132:34–44. [PubMed: 27353225]
36. Talcott KE, Ratnam K, Sundquist SM, et al. Longitudinal study of cone photoreceptors during retinal degeneration and in response to ciliary neurotrophic factor treatment. Invest Ophthalmol Vis Sci. 2011;52(5):2219–2226. [PubMed: 21087953]

37. Morgan JIW, Jiang YY, Vergilio GK, et al. Short-term assessment of subfoveal injection of adeno-associated virus–mediated hCHM gene augmentation in choroideremia using adaptive optics ophthalmoscopy. JAMA Ophthalmol. 2022;140(4):411–420. [PubMed: 35266957]
38. Patterson EJ, Kalitzeos A, Kasilian M, et al. Residual cone structure in patients with X-linked cone opsin mutations. Invest Ophthalmol Vis Sci. 2018;59(10):4238–4248. [PubMed: 30128495]
39. Patterson EJ, Wilk M, Langlo CS, et al. Cone photoreceptor structure in patients with X-linked cone dysfunction and red-green color vision deficiency. Invest Ophthalmol Vis Sci. 2016;57(8):3853–3863. [PubMed: 27447086]
40. Carroll J, Baraas RC, Wagner-Schuman M, et al. Cone photoreceptor mosaic disruption associated with Cys203Arg mutation in the M-cone opsin. Proc Natl Acad Sci U S A. 2009;106(49):20948–20953. [PubMed: 19934058]
41. McGee TL, Seyedahmadi BJ, Sweeney MO, Dryja TP, Berson EL. Novel mutations in the long isoform of the USH2A gene in patients with Usher syndrome type II or non-syndromic retinitis pigmentosa. J Med Genet. 2010;47(7);499–506. [PubMed: 20507924]
42. van Wijk E, Pennings RJ, te Brinke H, et al. Identification of 51 novel exons of the Usher syndrome type 2A (USH2A) gene that encode multiple conserved functional domains and that are mutated in patients with Usher syndrome type II. Am J Hum Genet. 2004;74(4):738–744. [PubMed: 15015129]
43. Ferris FL 3rd, Kassoff A, Bresnick GH, Bailey I. New visual acuity charts for clinical research. Am J Ophthalmol. 1982;94(1):91–96. [PubMed: 7091289]
44. Beck RW, Moke PS, Turpin AH, et al. A computerized method of visual acuity testing: adaptation of the early treatment of diabetic retinopathy study testing protocol. Am J Ophthalmol. 2003;135(2):194–205. [PubMed: 12566024]
45. BrainardLab. AOAutomontaging. Available at https://github.com/BrainardLab/AOAutomontaging/releases. Accessed December 20, 2022.
46. Rodieck RW. The density recovery profile: a method for the analysis of points in the plane applicable to retinal studies. Vis Neurosci. 1991;6(2):95–111. [PubMed: 2049333]
47. Nelder JA, Mead R. A simplex method for function minimization. Comput J. 1965;7(4):308–313.
48. McCulloch C, Searle S, Generalized Neuhaus J. Linear, and Mixed Models. 2nd ed. Hoboken, New Jersey: John Wiley & Sons; 2008.
49. Bland JM, Altman DG. Measuring agreement in method comparison studies. Stat Methods Med Res. 1999;8(2):135–160. [PubMed: 10501650]
50. Holm S. A simple sequentially rejective multiple test procedure. Scand J Stat. 1979;6(2):65–70.
51. Birch DG, Locke KG, Wen Y, Locke KI, Hoffman DR, Hood DC. Spectral-domain optical coherence tomography measures of outer segment layer progression in patients with X-linked retinitis pigmentosa. JAMA Ophthalmol. 2013;131(9):1143–1150. [PubMed: 23828615]
52. Abozaid MA, Langlo CS, Dubis AM, Michaelides M, Tarima S, Carroll J. Reliability and repeatability of cone density measurements in patients with congenital achromatopsia. Adv Exp Med Biol. 2016;854:277–283. [PubMed: 26427422]
53. Chen M, Cooper RF, Gee JC, Brainard DH, Morgan JIW. Automatic longitudinal montaging of adaptive optics retinal images using constellation matching. Biomed Opt Express. 2019;10(12):6476–6496. [PubMed: 31853412]
54. Garrioch R, Langlo C, Dubis AM, Cooper RF, Dubra A, Carroll J. Repeatability of in vivo parafoveal cone density and spacing measurements. Optom Vis Sci. 2012;89(5):632–643. [PubMed: 22504330]
55. Wang Y, Bensaid N, Tiruveedhula P, Ma J, Ravikumar S, Roorda A. Human foveal cone photoreceptor topography and its dependence on eye length. eLife. 2019;8:e47148. [PubMed: 31348002]

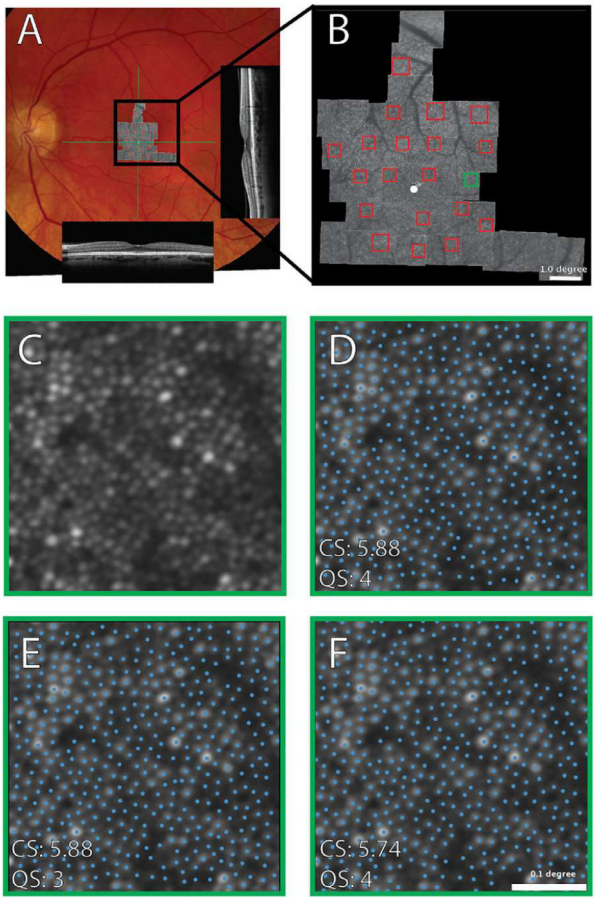

FIGURE 1.

A. Color fundus photograph with adaptive optics scanning laser ophthalmoscopy montage aligned using retinal vascular landmarks. Horizontal and vertical spectral-domain optical coherence tomography B-scans were acquired through the fovea at locations shown by green lines. B. Magnified adaptive optics scanning laser ophthalmoscopy montage with regions of interest (ROIs) shown in red boxes. The green box shows the ROI magnified in panels C through F. C. Cone mosaic at the ROI boxed in green in part B with cone profiles of varying reflectivity. D-F. Cones marked by 3 independent graders with cone spacing (CS, average nearest neighbor in arcminutes) values and quality score (QS) assessments by each grader shown. Scale bar = 0.1 degree.

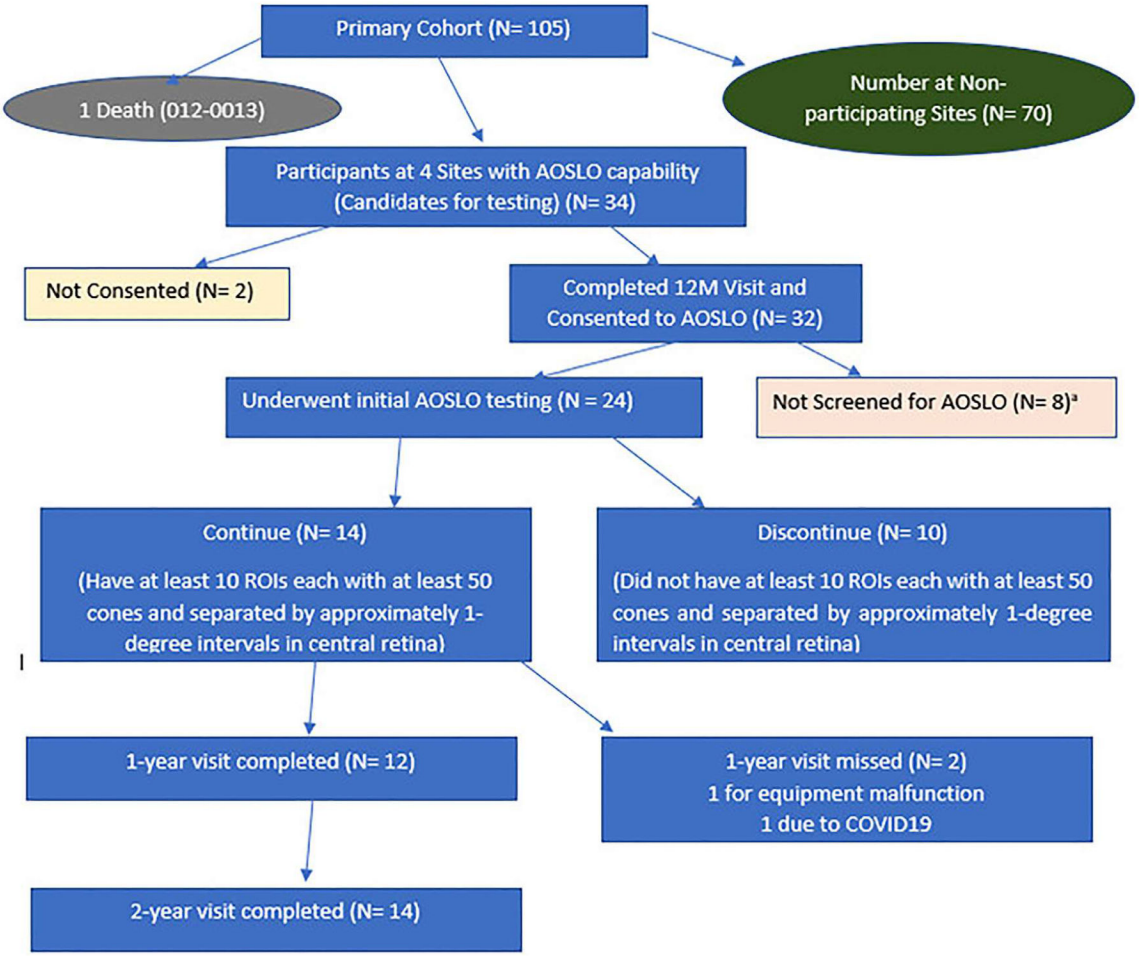

FIGURE 2.

Flow chart of Rate of Progression of *USH2A*-related Retinal Degeneration (RUSH2A) participant enrollment in adaptive optics scanning laser ophthalmoscopy (AOSLO) ancillary study. Eight of 34 participants screened at RUSH2A sites with AOSLO systems did not complete 2 baseline AOSLO montages as described in the text. Of 14 participants with ≥10 regions where ≥50 unambiguous cones were visible in contiguous mosaics separated by 1 degree, 12 completed the 24-month RUSH2A visit (12 months after baseline AOSLO imaging), while 14 completed the 36-month RUSH2A visit (24 months after baseline AOSLO imaging). ROI = region of interest.

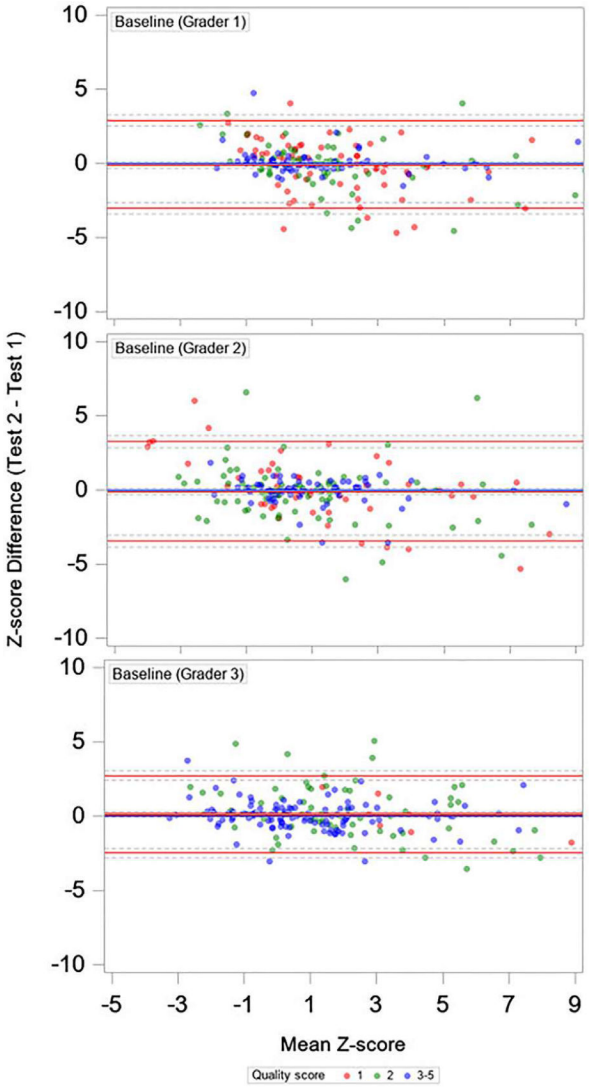

FIGURE 3.

Bland-Altman plots of cone spacing between baseline tests (Rate of Progression of *USH2A*-related Retinal Degeneration [RUSH2A] 12-month visit) by grader. Cone spacing Z-score measures at each region of interest at baseline were measured twice; the difference between the second measure (test 2) and the first (test 1) are shown on the Y-axis and plotted against the mean Z-score at each region of interest on the X-axis for each of 3 independent graders at baseline. Grader 1, top left panel; Grader 2, top right panel; Grader 3, bottom row. Image quality score for each ROI assessed by each grader is color coded as follows: 1 = red, 2 = green, and 3-5 = blue.

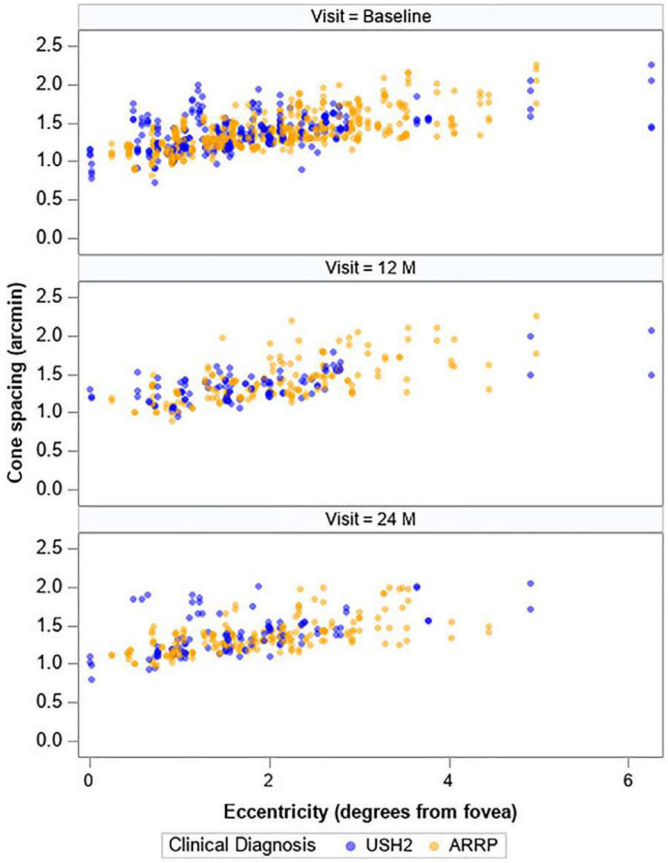

FIGURE 4.

Cone spacing compared with eccentricity from the fovea. Cone spacing (arcminutes, not converted to Z-score) increased with increasing distance from the fovea at each visit, and increased longitudinally over time. Cone spacing values for participants with Usher syndrome type 2 (USH2) are shown in blue, while values from participants with autosomal recessive retinitis pigmentosa (ARRP) are shown in orange. 12M = 12 months after baseline; 24M = 24 months after baseline.

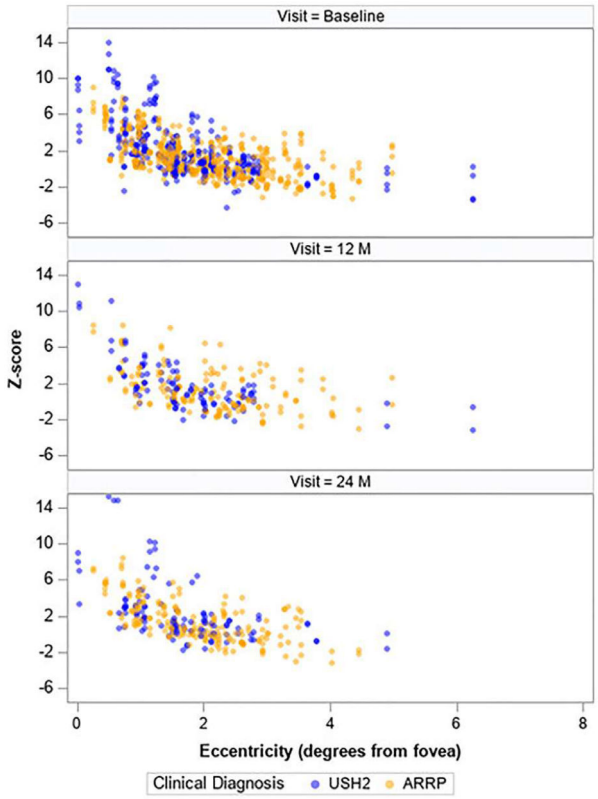

FIGURE 5.

Cone spacing (Z-score) compared with eccentricity from the fovea. Cone spacing (Z-score) decreased with increasing distance from the fovea at each visit, and increased longitudinally over time. Cone spacing values for participants with Usher syndrome type 2 (USH2) are shown in blue, while values from participants with autosomal recessive retinitis pigmentosa (ARRP) are shown in orange. 12M = 12 months after baseline; 24M = 24 months after baseline.

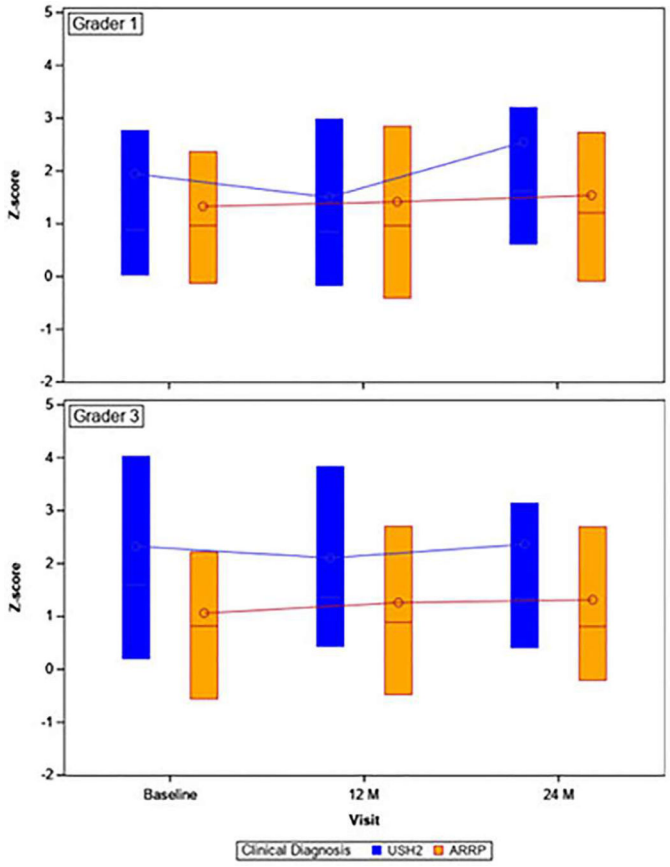

FIGURE 6.

Cone spacing Z-score compared with eccentricity over time, compared by grader and diagnosis. Cone spacing (Z-score) increased over time in both participants with Usher syndrome type 2 (USH2, shown in blue), and participants with autosomal recessive retinitis pigmentosa (ARRP, shown in orange). Mean values are shown as open circles connected by lines; median values are shown with lines, and interquartile range boundaries are shown with rectangles. 12M = 12 months after baseline; 24M = 24 months after baseline.

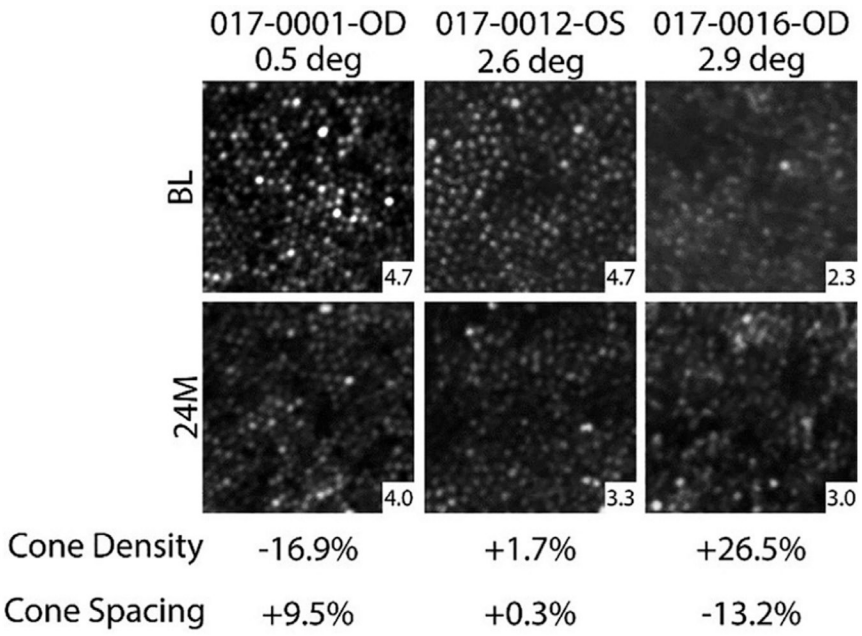

FIGURE 7.

Cone density change over 24 months. Shown are 3 regions of interest (ROIs) from 3 different participants representing examples of ROIs with an apparent decrease in cone density (left), minimal change in cone density (middle column), and an apparent increase in cone density (right) at the 24-month time point relative to baseline. In the example of an apparent increase in cone density, the lower image quality at baseline likely contributes to the paradoxical result, though small misalignments of the ROIs between timepoints can also contribute to errors in estimating the amount of change at a specific cone mosaic locus. The retinal eccentricity of each ROI is provided in degrees. The average quality score is on lower right of each image.

TABLE 1.

Baseline Participant Characteristics.

Characteristic	Overall	Clinical Diagnosis	
	N = 14	USH2, n = 6	ARRP, n = 8
Sex, n (%)			
Female	4 (29)	2 (33)	2 (25)
Male	10 (71)	4 (67)	6 (75)
Race/ethnicity, n (%)			
White	11 (79)	4 (67)	7 (88)
Hispanic	1 (7)	1 (17)	0
Asian	2 (14)	1 (17)	1 (13)
Enrollment area, n (%)			
United States/Canada	8 (57)	1 (17)	7 (88)
Europe/UK	6 (43)	5 (83)	1 (13)
Age at enrollment (y)			
Median (IQR)	38 (27-48)	31 (21-40)	46 (33-49)
[Min, Max]	[19, 59]	[19, 40]	[27, 59]
<35, n (%)	6 (43)	4 (67)	2 (25)
35-45, n (%)	4 (29)	2 (33)	2 (25)
≥45, n (%)	4 (29)	0	4 (50)
Age of onset (y)			
Median (IQR)	21 (14-42)	14 (13-20)	39 (21-45)
[Min, Max]	[8, 52]	[8, 21]	[14, 52]
<16, n (%)	6 (43)	4 (67)	2 (25)
16-25, n (%)	2 (14)	2 (33)	0
≥25, n (%)	6 (43)	0	6 (75)
Duration of disease (y)			
Median (IQR)	12 (6-16)	14 (11-19)	6 (4-14)
[Min, Max]	[1, 27]	[8, 27]	[1, 17]
<10, n (%)	6 (43)	1 (17)	5 (63)
10-19, n (%)	7 (50)	4 (67)	3 (38)
≥20, n (%)	1 (7)	1 (17)	0

ARRP = autosomal recessive retinitis pigmentosa; IQR = interquartile ratio; USH2 = Usher syndrome type 2.

TABLE 2.

Summary of Adaptive Optics Scanning Laser Ophthalmoscopy Measures From Baseline to 2-Years – Individual Grader Data

Outcomes	All[a]	Grader 1		Grader 2		Grader 3	
		USH2	ARRP	USH2	ARRP	USH2	ARRP
Baseline	**N = 1146, n = 14**	**N = 153, n = 6**	**N = 228, n = 8**	**N = 155, n = 6**	**N = 228, n = 8**	**N = 154, n = 6**	**N = 228, n = 8**
Z-score							
Mean (SD)	1.36 (2.55)	1.95 (3.04)	1.33 (2.13)	1.31 (2.51)	0.70 (2.23)	2.33 (3.07)	1.06 (2.24)
Median (IQR)	0.86 (−0.27 to 2.45)	0.88 (0.03-2.77)	0.96 (−0.13 to 2.37)	0.92 (−0.22 to 2.61)	0.26 (−0.56 to 1.70)	1.60 (0.20-4.03)	0.82 (−0.56 to 2.22)
Range	−4.37 to 13.95	−4.27 to 13.95	−2.40 to 8.96	−3.97 to 12.25	−4.37 to 8.72	−3.38 to 12.67	−3.30 to 7.95
Cone density (cones/mm^2)							
Mean (SD)	22,827 (8752.4)	25,402 (8153.9)	23,810 (9103.0)	23,380 (10221)	24,334 (9460.4)	19,772 (6041.5)	20,294 (7302.7)
Median (IQR)	21,457 (16,936-27,311)	24,435 (20,312-29,552)	22,207 (17,168-27,864)	21,615 (16,237-30,006)	23,033 (18,368-28,134)	19,161 (15,453-23,558)	19,332 (15,424-23,731)
Range	2252-64,616	10,007-64,616	8566-60,196	2252-62,074	6503-64,561	7921-37,410	4017-51,382
Cone spacing (arcmin)							
Mean (SD)	1.36 (0.23)	1.35 (0.26)	1.41 (0.25)	1.29 (0.22)	1.33 (0.21)	1.37 (0.19)	1.37 (0.21)
Median (IQR)	1.33 (1.20-1.48)	1.31 (1.18-1.51)	1.37 (1.23-1.56)	1.30 (1.13-1.43)	1.30 (1.19-1.43)	1.37 (1.22-1.51)	1.33 (1.23-1.46)
Range	0.72-2.26	0.72-2.26	0.83-2.20	0.79-2.10	0.81-2.20	0.87-1.78	0.90-2.26
1 year	**N = 254, n = 12**	**N = 45, n = 12**	**N = 78, n = 12**			**N = 53, n = 12**	**N = 78, n = 12**
Z-score							
Mean (SD)	1.53 (2.57)	1.50 (2.41)	1.42 (2.47)			2.11 (3.16)	1.26 (2.29)
Median (IQR)	1.09 (−0.24 to 2.90)	0.85 (−0.17 to 2.99)	0.96 (−0.41 to 2.85)			1.36 (0.43-3.83)	0.89 (−0.48 to 2.70)
Range	−3.13 to 12.95	−1.57 to 10.83	−2.67 to 8.43			−3.13 to 12.95	−2.96 to 8.49
Cone density (cones/mm^2)							
Mean (SD)	20,173 (7830.6)	23,263 (7385.6)	20,540 (8800.0)			19,763 (6516.6)	18,301 (7402.7)
Median (IQR)	19,028 (14,529-23,954)	22,766 (18,091-28,586)	18,453 (14,152-24,072)			18,597 (14,330-24,224)	17,563 (12,146-22,512)
Range	4682-52,298	9064-38,227	8038-52,298			8411-32,406	4682-47,411
Cone spacing (arcmin)							
Mean (SD)	1.39 (0.25)	1.35 (0.22)	1.43 (0.29)			1.35 (0.22)	1.43 (0.29)

Outcomes	All[a]	Grader 1		Grader 2		Grader 3	
		USH2	ARRP	USH2	ARRP	USH2	ARRP
Baseline	**N = 1146, n = 14**	**N = 153, n = 6**	**N = 228, n = 8**	**N = 155, n = 6**	**N = 228, n = 8**	**N = 154, n = 6**	**N = 228, n = 8**
Median (IQR)	1.36 (1.22-1.49)	1.32 (1.20-1.43)	1.37 (1.24-1.62)			1.32 (1.20-1.43)	1.37 (1.24-1.62)
Range	0.89-2.26	0.95-2.07	0.89-2.26			1.01-1.80	0.99-2.20
2-year	**N = 261, n = 14**	**N = 51, n = 14**	**N = 62, n = 14**			**N = 55, n = 14**	**N = 93, n = 14**
Z-score							
Mean (SD)	1.80 (2.78)	2.55 (3.50)	1.54 (2.39)			2.37 (3.33)	1.31 (2.21)
Median (IQR)	1.22 (0.01-2.92)	1.62 (0.61-3.21)	1.21 (−0.09 to 2.73)			1.35 (0.41-3.14)	0.81 (−0.21 to 2.70)
Range	−3.12 to 15.27	−1.31 to 14.87	−3.12 to 8.42			−1.71 to 15.27	−3.05 to 7.76
Cone density (cones/mm^2)							
Mean (SD)	21,835 (8334.0)	23,578 (8802.1)	22,314 (9072.1)			21,371 (8046.3)	20,674 (7339.6)
Median (IQR)	20,411 (15,983-26,765)	22,645 (17,622-28,644)	20,611 (15,771-27,252)			20,285 (15,137-27,040)	19,307 (15,845-24,393)
Range	8082-55,206	9737-44,948	8082-55,206			8828-40,767	8544-46,887
Cone spacing (arcmin)							
Mean (SD)	1.37 (0.23)	1.38 (0.27)	1.37 (0.24)			1.37 (0.26)	1.35 (0.19)
Median (IQR)	1.33 (1.20-1.46)	1.35 (1.18-1.50)	1.34 (1.20-1.44)			1.30 (1.18-1.55)	1.32 (1.22-1.43)
Range	0.80-2.04	0.80-2.04	0.97-2.00			0.95-2.02	1.00-2.00

IQR = interquartile range; SD = standard deviation.

[a]N indicates the number of region of interest gradings; n is the number of participants.

TABLE 3.

Summary of Adaptive Optics Scanning Laser Ophthalmoscopy Measures from Baseline to 2 Years of Follow-Up

Outcomes	Baseline[a]			12 Months[a]			24 Months[a]		
	Overall (N = 763)	USH2 (n = 307)	ARRP (n = 456)	Overall (N = 254)	USH2 (n = 98)	ARRP (n = 156)	Overall (N = 292)	USH2 (n = 106)	ARRP (n = 186)
Z-score									
Mean (SD)	1.57 (2.61)	2.14 (3.05)	1.20 (2.19)	1.53 (2.57)	1.83 (2.84)	1.34 (2.37)	1.80 (2.78)	2.45 (3.40)	1.42 (2.29)
Median (IQR)	1.02 (−0.16 to 2.67)	1.39 (0.12-3.43)	0.91 (−0.26 to 2.34)	1.09 (−0.24 to 2.90)	1.18 (−0.08 to 3.07)	0.95 (−0.44 to 2.75)	1.22 (0.01-2.92)	1.52 (0.44-3.14)	0.99 (−0.20 to 2.73)
Range	−4.27 to 13.95	−4.27 to 13.95	−3.30 to 8.96	−3.13 to 12.95	−3.13 to 12.95	−2.96 to 8.49	−3.12 to 15.27	−1.71 to 15.27	−3.12 to 8.42
Cone density (cones/mm^2)									
Mean (SD)	22,264 (8140.8)	22,578 (7695.8)	22,052 (8428.9)	20,173 (7830.6)	21,370 (7112.1)	19,420 (8182.7)	21,835 (8334.0)	22,433 (8450.9)	21,494 (8270.1)
Median (IQR)	20,926 (16,702-26,631)	21,314 (17,061-27,174)	20,595 (16,533-26,184)	19,028 (14,529-23,954)	20,759 (16,119-25,788)	17,985 (13,613-23,472)	20,411 (15,983-26,765)	21,404 (16,708-27,576)	19,819 (15,771-26,063)
Range	4017-64,616	7921-64,616	4017-60,196	4682-52,298	8411-38,227	4682-52,298	8082-55,206	8828-44,948	8082-55,206
Cone spacing (arcmin)									
Mean (SD)	1.38 (0.23)	1.36 (0.23)	1.39 (0.24)	1.39 (0.25)	1.35 (0.19)	1.42 (0.27)	1.37 (0.23)	1.38 (0.26)	1.36 (0.22)
Median (IQR)	1.35 (1.22-1.50)	1.34 (1.20-1.51)	1.35 (1.23-1.50)	1.36 (1.22-1.49)	1.34 (1.21-1.45)	1.37 (1.23-1.57)	1.33 (1.20-1.46)	1.33 (1.18-1.51)	1.33 (1.21-1.43)
Range	0.72-2.26	0.72-2.26	0.83-2.26	0.89-2.26	0.95-2.07	0.89-2.26	0.80-2.04	0.80-2.04	0.97-2.00

ARRP = autosomal recessive retinitis pigmentosa; IQR = interquartile ratio; SD = standard deviation; USH2 = Usher syndrome type 2.

[a]N indicates the number of region of interest (ROI) gradings; 12M, 12-month visit; 24M, 24-month visit.

TABLE 4.

Regions of Interest and Image Quality Scores.

	Baseline (N = 14)	12 Months[a] (N = 12)	24 Months (N = 14)
ROIs, n (%)			
<10	N/A	5 (42)	4 (31)
10	3 (21)	1 (8)	2 (15)
11-15	7 (50)	4 (33)	4 (31)
>15	4 (28)	2 (17)	3 (23)
ROIs lost from baseline, n (%)			
0	N/A	2 (17)	6 (46)
1-3	N/A	6 (50)	3 (23)
4-7	N/A	4 (33)	4 (31)
Average quality score (SD)			
Baseline ROIs 10	2.17 (0.21)	1.70 (0.28)	1.33 (0.64)
Baseline ROIs 11-15	2.29 (0.56)	1.94 (0.96)	2.07 (0.77)
Baseline ROIs >15	3.05 (0.60)	3.37 (0.55)	2.90 (0.39)

N/A = not applicable; ROI = region of interest; SD = standard deviation.

[a]Two participants missed the 12-month visit.

TABLE 5.

Association Between Cone Spacing Z-Score and Participant Characteristics at Baseline (Graders 1 and 3 Only)

	Z-Score		
	Model Estimate (Weighted)	**Univariate *P* Value**	**Adjusted *P* Value[a]**
Clinical diagnosis (ARRP)	−1.40	.21	
Male sex	−0.41	.75	
Grader	−0.09	.21	
Test number	0.04	.56	
Site	−0.27	.13	
Eccentricity (degree)	−1.21	<.001[b]	<.001[b]
Quality score	−0.18	.008[b]	,004[b]
Disease duration, years	0.19	.007[b]	.02[b]
No. of regions of interest	−0.22	.14	

AARP = autosomal recessive retinitis pigmentosa.

[a]Models take into account quality scores by weighting the data using reciprocal of the root mean square between graders. Adjusted *P* value is from a multivariable model including quality score, disease duration, and number of regions of interest.

[b]$P < .05$.

TABLE 6.

Estimated Average Annual Change Based on Random Intercept Models (Weighted)

Outcomes	Z-Score	
	Entire Cohort (N = 14, n = 1309)	**Univariate *P* Value[a]**
Cone spacing		
Annual change (95% CI)	0.14 (0.07-0.21)	<.001
No. of regions of interest		
Annual change (95% CI)	−0.18 (−0.23 to −0.12)	<.001

CI = confidence interval.

[a]Results remain similar when adjusting for clinical diagnosis.

TABLE 7.

Spearman Correlation Coefficients (**95% C**onfidence Intervals) Betw**een Z**-Score **and** Other Measurements **at** Baseline **and** Between Change **in Z**-Score With Cha**nge in** Other Measurements

	Spearman Correlation Coefficient					
	Cross-Sectional		Change in Z-Score With Change in Measures			
	Baseline		1-Year[a]		2-Year[b]	
	r	Adjusted *P* Value[c]	r	Adjusted *P* Value[c]	r	Adjusted *P* Value[c]
BCVA (within 1 degree)	−0.68	.97	0.48	.75	0.21	1
FST white	0.59	.63	−0.48	.78	−0.67	.24
FST blue	0.54	.66	−0.48	.78	−0.53	.61
FST red	0.44	.97	−0.48	.78	−0.02	1
Ellipsoid zone area	−0.46	.63	−0.05	.90	−0.22	1
MP mean sensitivity	−0.28	.97	0.50	.60	0.19	1

BCVA = best-corrected visual acuity; FST = full-field stimulus threshold; MP = microperimetry.

[a]Spearman correlation coefficients for change in adaptive optics scanning laser ophthalmoscopy measures with change in all visual outcomes from baseline to 12 months.

[b]Spearman correlation coefficients for change in adaptive optics scanning laser ophthalmoscopy measures with change in all visual outcomes from baseline to 24 months.

[c]Adjusted for multiple comparisons.